Interactions between Molten Aluminum and Various Refractory Materials

V. Schönhof, W. Schönwelski, J. Sperber, M. Bay

Different interactions between molten aluminum (AlMg5-alloy) and various refractory materials are investigated by crucible tests. The test samples were analyzed by:

- Macroscopic investigation
- Microscopic investigation
- scanning electron microscope (SEM)
- X-ray diffraction (XRD).

Corrosion mechanisms and reaction products were studied. Results show that the most important criterion for SiC-bricks is the binding system. Silicate-bonded products show intense infiltration. In contrast nitride-bonded SiC proved to be very resistant against molten aluminum.

The investigation shows that the resistance of alumosilicate materials depends on the SiO_2 content of the brick. Accordingly, the corrosion resistance of bauxite bricks is better compared to andalusite bricks. High-purity corundum are resistant to Al-melts, but because of the porosity mechanical infiltration takes place related to porosity. The formation of spinel could not be confirmed

1 Introduction

This paper is based on the paper published by Schoenwelski, et al. [1] and tries to describe the reaction processes and products more detailed to get results for application. Standard refractory products were tested as well as new material compositions (Tab. 1). Simultaneously such parameters as dwelling times and test temperatures have been varied.

Most of the bricks which were tested contain SiO_2. In contact with molten aluminum SiO_2-containing refractory bricks it can be expected that the SiO_2 is reduced by aluminum. In this context the Jeffes-Richardson-Diagram (Fig. 1) gives significant information. This diagram shows the enthalpy of formation ΔG as a function of temperature. The graphs of noble/precious metals are located over the graphs of less noble metals, which have a higher oxygen affinity and therefore suitable as a reducing medium. Consequently the stability of the oxide increases with lower ΔG values. It is known that SiO_2 (red graph in Fig. 1) is reduced by the presence of molten aluminum [14]:

$4Al + 3\,SiO_2 \rightarrow 2\,Al_2O_3 + 3Si$

Our aim was to investigate the corrosion mechanisms between molten aluminum and different refractory materials and to investigate the resulting components.

Tab. 1 Overview of the aluminum tests (all tests in reducing atmosphere)

Name	Quality	Tests Carried out
SC 90	Silicate-bonded SiC-brick	850 °C/1100 °C
SCN 70	Nitride-bonded SiC-brick	850 °C/1100 °C/ 320 h at 900 °C
B 80	Fired bauxite brick containing phosphate	850 °C/1100 °C/ 320 h at 900 °C
SA	Fired andalusite brick	850 °C/1100 °C
K 99	Direct-bonded corundum brick	850 °C/1100 °C

2 Results Analysis

For the tests the crucibles were covered with graphite foil and a lid to prevent the oxidation of the Al-melt. The test temperatures were 850 °C and 1100 °C. After a dwelling time of 72 h the molten aluminum has been poured out. Some tests were executed at 360 h (Tab. 1).

2.1 Macroscopic Analysis

Tab. 2 presents the results in detail.

SC 90: Crucible test with SC 90 (silicate bonded SiC) (Fig. 2) shows a circular infiltration of 14 mm depth. The metallic reflection of this area suggests a mechanical infiltration. Compared to the rest this zone is denser. Especially when temperature changes take place the densification may result in spalling [9]. Knowing that the SiC component is proved to be stable, an alternative binding system for silicate binding is preferred.

Viktor Schönhof, Werner Schoenwelski, Jens Sperber, Markus Bay
Steuler-KCH GmbH
56203 Höhr-Grenzhausen
Germany

Corresponding author: *Viktor Schönhof*
E-mail: *v.schoenhof@steuler-kch.de*

Keywords: aluminium, refractories, nitride bond

Journal of Ceramic Science and Technology 5 (2014) [2]

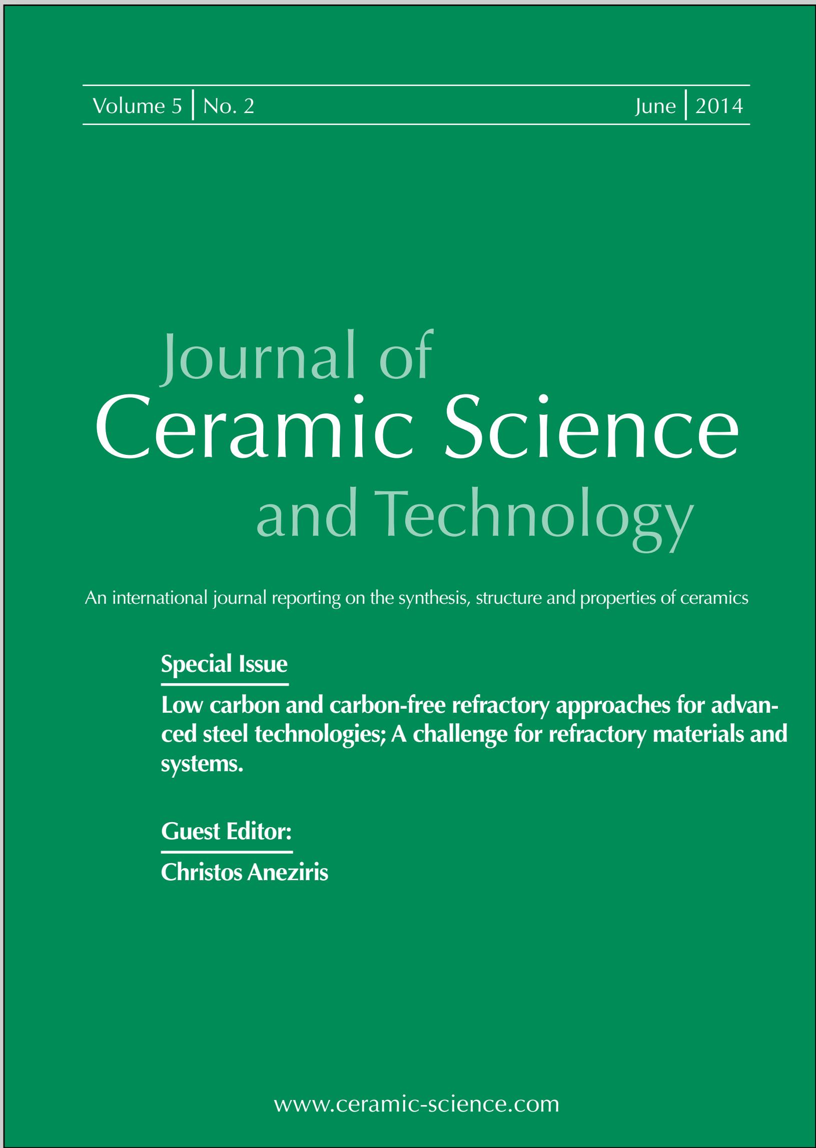

Special Issue:
Low carbon and carbon-free refractory approaches for advanced steel technologies; A challenge for refractory materials and systems.

Guest Editor:
Christos Aneziris

Price:
EUR 98,–

First „Open Access“ issue of the „Journal of Ceramic Science and Technology“ supported by the German Science Foundation (DFG).
Volume 5, Issue 2 is now available on: http://www.ceramic-science.com

German Ceramic Society
Bergerstraße 145a, D-51145 Köln
Phone: +49 (0) 2203-9898770
Fax: +49 (0) 2203-9898779
Internet: www.dkg.de, E-mail: info@dkg.de

Göller Verlag – publisher of refractories WORLDFORUM, Journal of Ceramic Science and Technology (JCST)

www.ceramics-science.com

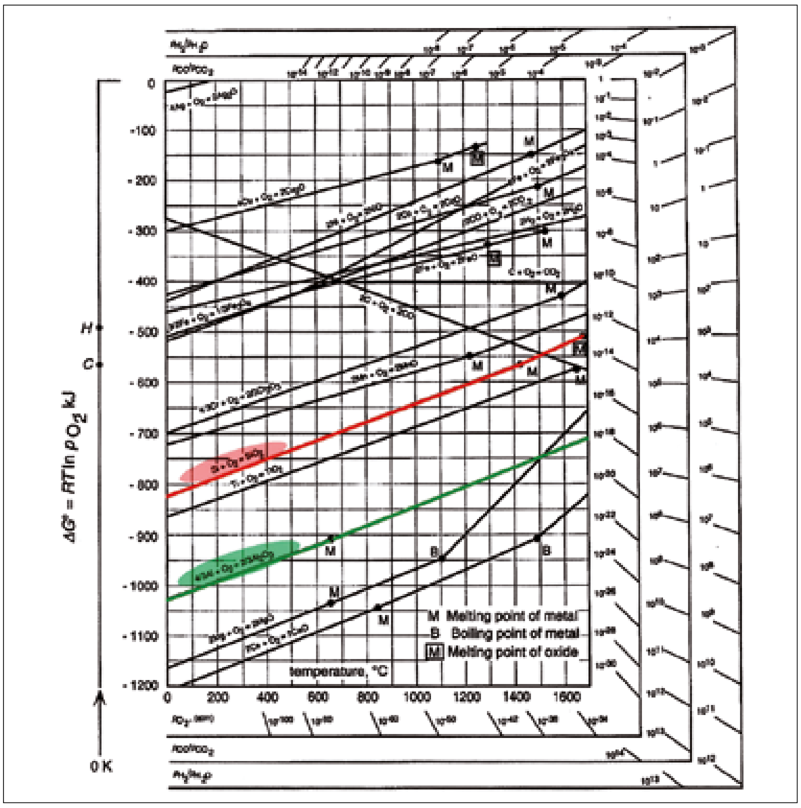

Fig. 1 The Jeffes-Richardson-Diagramm [10] shows the enthalpy of formation ΔG as a function of temperature. It describes the thermodynamic stability of oxides, which increases with lower ΔG values. It is known that SiO_2 (red graph) is reduced by the presence of molten aluminum.

SCN 70: According to literature a Si_3N_4- or Si_2ON_2 bound SiC-bricks have good resistance against molten aluminum [10]. We tested our nitride bonded quality SCN 70. In contrast to the SC 90 the SCN 70 (nitride bonded SiC) (Fig. 3) has a very high corrosion resistance. No structure changes and no infiltration can be observed. After pouring off the melt, the aluminum skin can be detached from the crucible surface and there has been no wetting. Spare literature information about the contact angle θ of aluminum on Si_3N_4 substrates confirms the test results (Fig. 4). The critical temperature (θ < 90 °) of Si_3N_4 is estimated to be about 1000 °C.

To characterize the wetting behavior of SCN 70 an Al-test at 1100 °C was carried out (Fig. 5). After pouring, the aluminum can peeled off only on certain areas. The infiltration depth is 2 mm. This supports the assumption that for this variation the wetting behavior between 800 – 1100 °C shows significant differences. One can also see that between aluminum and brick material a black seam has formed (see image magnification). Confirmed by literature [5, 10] an AlN barrier layer has formed. The following reaction takes place:

$Si_3N_4 + 4Al \rightarrow 4AlN + 3Si$

The very low corrosion and the formation of a protective layer of aluminum nitride shows that silicon nitride is a suitable corrosion protection material when handling molten aluminum [7].

Tab. 2 Comparison of infiltration depths of the investigated qualities

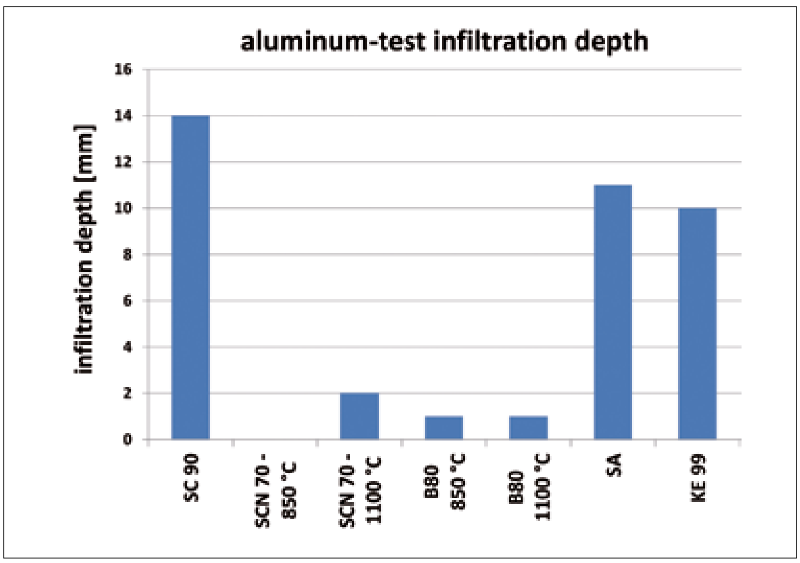

B 80: The test of B 80 (fired bauxite brick containing phosphate) (Fig. 6) shows that there are no differences of corrosion behaviour between the 850 °C and 1100 °C test. This shows that bauxite bricks can be exposed higher temperature fluctuations in the aluminum industry.

An infiltration depth of 1 mm can be seen. In this zone a chemical reaction between the components and aluminum takes place. Al_2O_3 was built by reaction of aluminum with the SiO_2-containing matrix of the bauxite brick [14]:

$4\,Al + 3\,SiO_2 \rightarrow 2\,Al_2O_3 + 3\,Si$

This effect is called „intern corundum growth". The resulting silicon is partly absorbed by the molten aluminum as an alloy component.

SA: At the crucible test with SA (fired andalusite brick) (Fig. 7) a corrosion attacked and densified zone with a depth of 11 mm can be seen. Along the border of reaction layer and the structure a crack has appeared. This will unavoidably lead to spalling, which results in a rapid loss of material.

K 99: The black infiltrated zone observed in the test of K 99 (direct bonded corundum brick) could be suspected to be related to spinel formation (generated by the Mg-content of the alloy) or just a mechanical infiltration. Literature mentions a wetting angle θ for aluminum on corundum of

Fig. 2 Al-crucible test of SC 90, dwelling time: 72 h, temperature: 850 °C

Fig. 3 Al-crucible test of SCN 70, dwelling time: 72 h, temperature: 850 °C

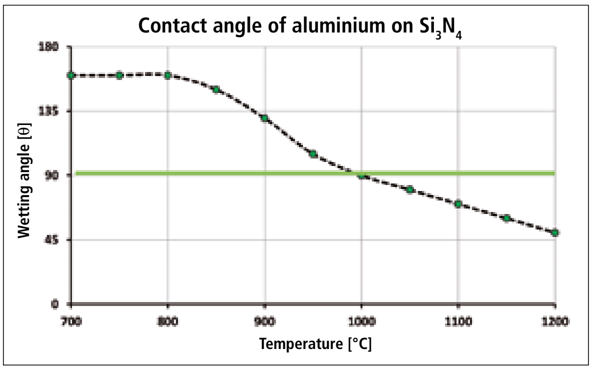

Fig. 4 Wetting angle θ as a function of temperature [11]. The transition from non-wetting to wetting (θ = 90°) is for Si_3N_4 at about 1000 °C.

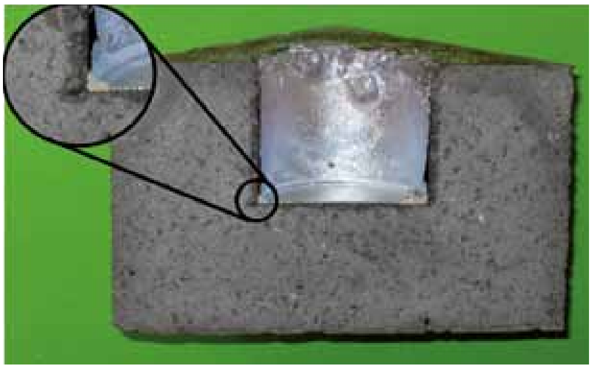

Fig. 5 Al-crucible test of SCN 70, dwelling time: 72 h, temperature: 1100 °C

Fig. 6 Al-crucible test of B 80, dwelling time: 72 h, temperature: 850 °C

Fig. 7 Al-crucible test of SA, dwelling time: 72 h, temperature: 850 °C

about 90–120° [3, 12, 15]. At the three-phase boundary a material growth occurred (Fig. 8).

Oxidizing of molten aluminum in the bath area by building corundum is called "external corundum growth" by literature [4, 14], described by following simple reaction:

$4\,Al + 3\,O_2 \rightarrow 2\,Al_2O_3$

In literature it is pointed out that if Mg is present (from the alloy $AlMg_5$) spinel ($MgAl_2O_4$) can form [8, 14]. This assumption cannot be confirmed by our investigations, see below.

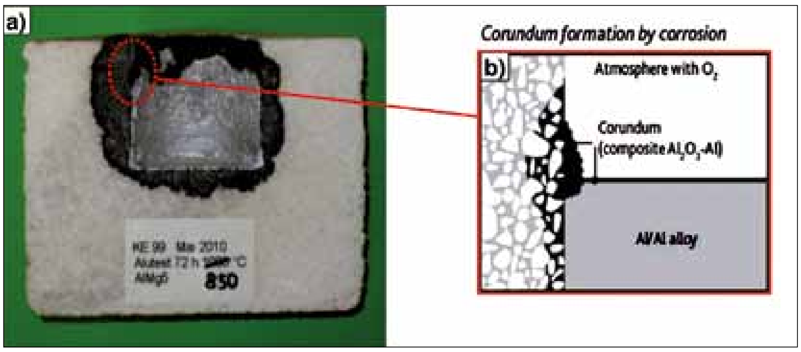

Fig. 8 Al-crucible test of K 99, dwelling time: 72 h, temperature: 850 °C, schematic of the „corundum growth" [8]

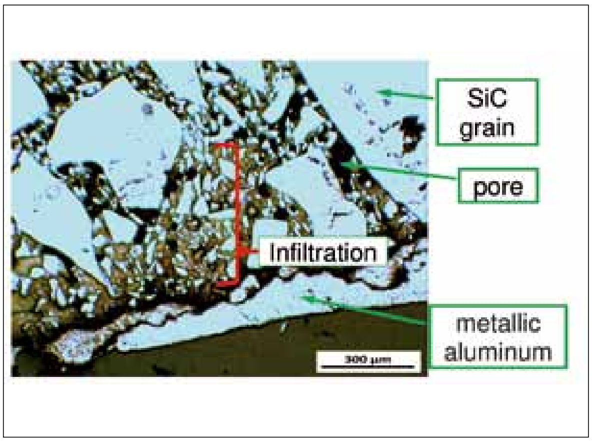

Fig. 9 LM-micrograph of Al-test of SC 90

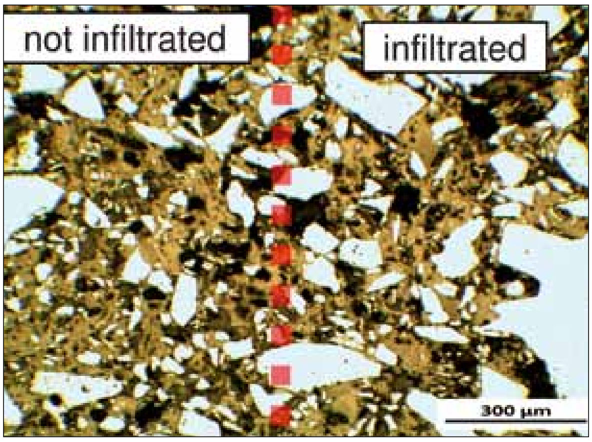

Fig. 10 LM-micrograph of Al-test of SCN 70 (1100 °C, 72 h)
The red marker indicates the macroscopically visible transition from infiltrated and non-infiltrated area. This transition is microscopically not visible.

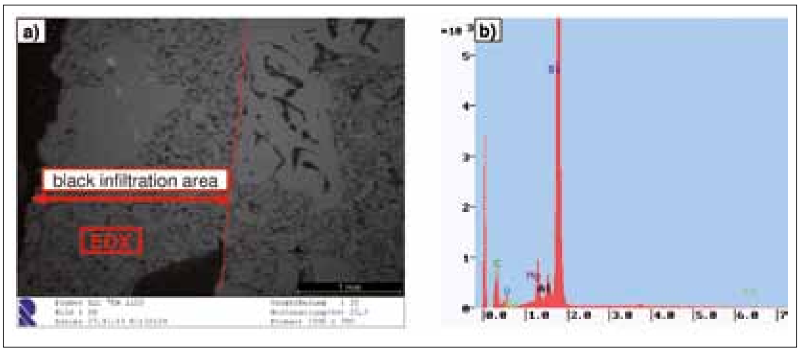

Fig. 11 SEM and EDX analysis of SCN 70 Al-test:
a) the red marker indicates the transition from infiltration and not infiltrated structure; there is no difference visible;
b) EDX analysis of the black infiltration area. The presence of Mg and Al indicates that the Al melt must be infiltrated.

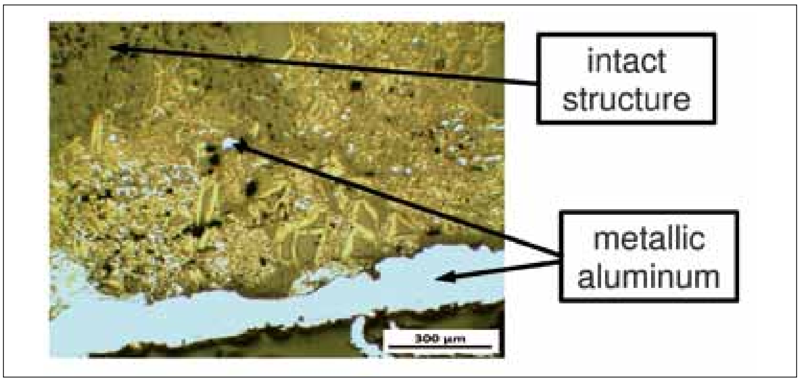

Fig. 12 LM-micrograph of Al-test of B 80 (1100 °C, 72 h)

2.2 Microscopy and scanning electron microscope (SEM)

SC 90: The microscopic analysis of SC 90 (Fig. 9) shows that the SiC-grains are not attacked. It is striking that the infiltrated matrix reflects different from metallic aluminum. This indicates that the matrix, consisting of SiO_2, has reacted with the infiltrated aluminum. Microscopic pictures of SCN 70 from the boundary area confirm that aluminum has not wetting to Si_3N_4-bound SiC-bricks. There is no infiltration of aluminum visible. In Fig. 10 the macroscopically indicated transition (see magnification in Fig. 5) of infiltrated area (right half) and not infiltrated area (left half) is shown. This transition is microscopically in Fig. 10 undetectable. It can be concluded that the particle size of the infiltrated aluminum for light microscopy is too small. It is also possible that the reaction products have to small contrast effects for light microscopy.

SCN 70: The SEM-picture (Fig. 11) of SCN 70 also does not show any reaction or infiltration. EDX-analysis of the infiltrated area shows that the elements Al and Mg are present. This necessarily implies that molten aluminum must have infiltrated in small amounts.

B 80: The microscopic analysis of aluminum test with B 80 (Fig. 12) clearly shows that the matrix has reacted in the infiltration area. Here the grain structure of the matrix is easy to distinguish. The attack on corundum grains by forming a reaction rim can be seen. Small bright reflecting surfaces are visible, which implies that there has been a mechanical infiltration of aluminum. The SEM-analysis of B 80 (Fig. 13) shows that the infiltrated zone is much denser than the rest of the structure. Both areas were analyzed by EDX and the comparison shows that in the infiltrated area Mg is present, but less Si is found. It can be concluded that a spinel formation has taken place in the infiltrated area. The EDX analysis of the infiltrated area has a significantly lower P-content, which means that in this area less aluminum phosphate is present. The transformation of aluminum phosphate in the presence of Al to Al_2O_3 is confirmed in literature and takes place under the follows equation [2]:

$5\,Al + 3\,AlPO_4 \rightarrow 4\,Al_2O_3 + 3\,P$

The less Si content in the infiltrated area shows that the components reacted to corundum.

The free Si and P will be included from the molten Al as an alloy component. In summary, it is clear that by forming a dense layer a corundum growth takes place, preventing further corrosive reactions.

SA: The micrograph (Fig. 14) of the SA-tests confirms the low resistance of the andalusite against molten aluminum. It can be seen that the structure has reacted with the infiltrated melt. Because of the transformation of andalusite to mullite + SiO_2 it can be assumed that the resulting reaction product is an internal corundum growth [14]. The high SiO_2 content of andalusite brick is the reason for intensive corrosion. The magnesium content in the aluminum alloy ($AlMg_5$) enables the formation of the spinel. The following reaction takes place [6]:

$3\,Mg + 4\,Al_2O_3 \rightarrow 3\,Mg\,Al_2O_4 + 2\,Al$

K 99: The magnification image of the microscope picture of the K 99 (Fig. 15) shows that the corundum structure was not attacked. The fine-grained bright reflective phase between the individual grains indicates a mechanical infiltration of the metallic aluminum, which has not reacted with the corundum. The infiltration of open porosity is very important for the corrosion process.

The reduction of porosity of corundum bricks is limited if thermal shock resistance is required. This indicates a limited suitability of corundum bricks in aluminum melting industries.

2.3 X-ray diffraction (XRD)

Tab. 3 presents the results in detail.

SC 90: The RBA of the SC 90 confirms that the SiC grain is not affected by the metallic aluminum. Striking is the significant presence of Al_2O_3, which can be explained by the exothermic reaction and the high oxygen affinity of Al. A further reason for the formation of Al_2O_3 is the reduction of the SiO_2 oxide layer. This is confirmed by the absence of SiO_2 and the low content of Si [13].

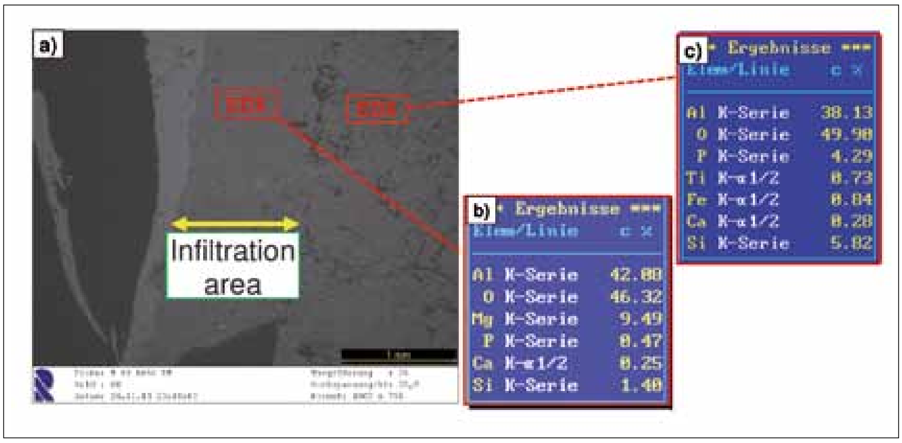

Fig. 13 SEM and EDX analysis of B 80 Al-test (850 °C):
a) SEM image; b) EDX analysis of the infiltrated area; c) EDX analysis of the structure

The silicate bonding phase of SC 90 proves to be not resistant in contact with molten aluminum.

SCN 70: The XRD of SCN 70 doesn't indicate Al or Mg. A possible explanation for the absence of these compounds is that their amount is below the detection limit. Thus, the blackening of the infiltration area could be due to a particle size effect of the infiltrated aluminum. It can be seen that both the SiC grain structure and the binding phases (Si_3N_4 and Si_2ON_2) are resistant to aluminum melt.

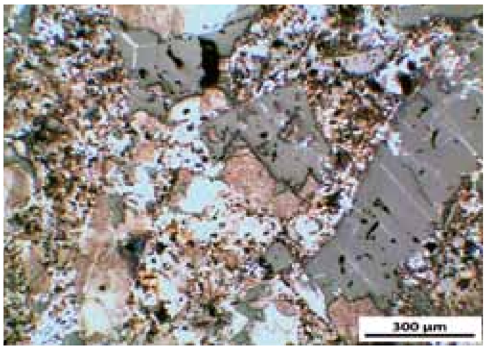

Fig. 14 LM-micrograph of Al-test of SA (850 °C, 72 h)

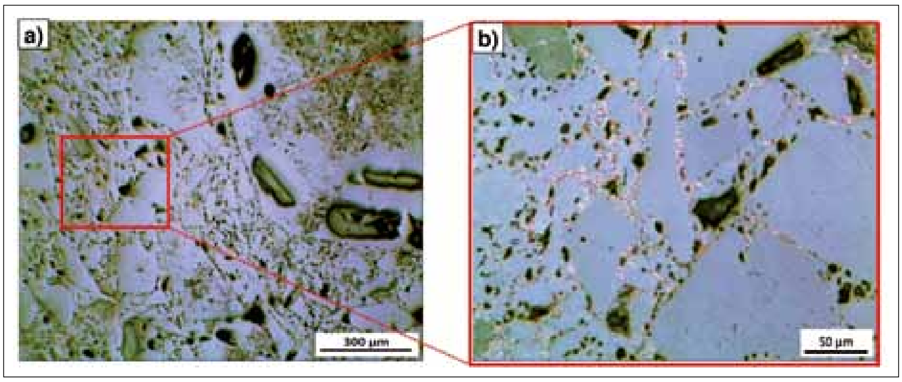

Fig. 15 LM-micrograph of Al-test of K 99 (850 °C, 72 h)

Tab. 3 Overview of the XRD of the infiltrated/reacted areas

Investigated Quality	Main Phase	Low Proportion	Traces
SC 90	SiC	Al_2O_3	Si, Al
SCN 70	SiC	Si_3N_4	Si_2ON_2
B 80	Al_2O_3 Al_4SiO_5 (Mullite)	$MgAl_2O_4$ (Spinel) $AlPO_4$ (Berlinite)	SiO_2 (Cristobalite)
SA	Al_2O_3 Al_2SiO_5 (andalusite)	$3\,Al_2O_3$* $2\,SiO_2$ (Mullite) $MgAl_2O_4$ (Spinel)	Si
K 99	Al_2O_3 (Corundum)	–	–

Tab. 4 Conclusions of the aluminum tests

Name	Raw Material Base	Type of Corrosion		Stable Phase	New Phase	Suitability	Comment
		Infiltration	Formation of New Phases				
SC 90	SiC SiO_2-binding	XXX	yes	SiC	Al_2O_3	limited	Contra: SiO_2-formation
SCN 70	SiC Si_3N_4 + SI_2ON_2-binding	–	no	SiC, Si_3N_4, SI_2ON_2	–	yes	Pro: high resistance Contra: production costs
B 80	Bauxite, Al-phosphate	X	yes	Al_2O_3, berlinite	Al_2O_3 spinel	yes	Pro: less corrosion and less production costs
SA	Andalusite	XX	yes	–	Corundum, spinel	no	
K 99	Corundum	XX	no	Corundum	–	limited	Infiltration because of too high porosity

B 80: The XRD of B 80 confirms the results in the SEM-analysis of the formation of spinel in the infiltration area. The presence of berlinite ($AlPO_4$) and the added phosphate binder promotes the transformation to a very dense corundum layer. This prevents further infiltration of aluminum melt. At the same time a progressive reaction is prevented because of the created layer. The aluminum has no further contact with the SiO_2-containing bauxite brick structure.

SA: The result of XRD of the test with SA confirms the transformation of andalusite to mullite. The presence of spinel shows that the alloy compound Mg participated in the reaction [6].

Concluding the SA-test it is very clear that a higher SiO_2 content in the raw materials causes a decrease in the corrosion resistance of Alumosilicate products.

K 99: The result of the XRD of K 99 confirms the reaction resistance of corundum against molten Al. The basis for the macroscopically recognizable infiltration is the penetration of molten aluminum into the open porosity of the brick. Al was not detected by XRD because the infiltration amount is below the detection limit. The X-ray diffraction analysis makes it clear that the formation of spinel based to the alloy component Mg has not taken place under the experimental conditions.

3 Summary

The results of the corrosion tests using an Al-Mg5-alloy are summarized as follows. For SiC-bricks the binding system is a crucial factor for the resistance to molten aluminum. In contrast to the high infiltration of the silicate-bonded SC 90 the nitride-bonded SCN 70 could bring out its resistance against all other tested bricks. This quality has a very promising application in the aluminum industry.

The selection of alumosilicate materials has shown that the SiO_2 content is as crucial to the resistance of corrosive attack. Accordingly, the corrosion resistance of bauxite brick (B 80) is better compared to andalusite brick (SA). In addition, the presence of berlinite ($AlPO_4$) proves to be a corrosion inhibitor. High-purity corundum bricks have been identified as resistant to Al melts. Occurring mechanical infiltration is dependent on porosity.

References

[1] Schoenwelski, W.; Sperber, J.; Bay, M.: Non-oxidic binding systems of refractory products for metal melts. refractories WORLDFORUM **3** (2013) 73–76

[2] Adabi Firoozjaei, E.; Koshy, P.; Sorrell, C.C.: Effects of $AlPO_4$ addition on the corrosion resistance of andalusite-based low-cement castables with molten Al-alloy, J. Europ. Ceram. Soc. **33** (2013) 1067–1075

[3] Aguilar-Santillan, J.: Wetting of Al_2O_3 by molten aluminum: The influence of $BaSO_4$ additions. J. of Nanomater. (2008), Article ID 629185, 12 pages

[4] Allaire, C.; Guermatzi, M.: Effect of several parameters on corundum growth in aluminium treatment furnaces. J. Canadian Cer. Soc. **69** (2000) [2] 3135

[5] Kollenberg, W.: Technische Keramik. Essen 2004

[6] McLeod, A.D.; Gabryel, C.M.: Kinetics of the growth of spinel, $MgAl_2O_4$, on alumina particulate in aluminum alloys containing magnesium. Metallurgical Trans. **23** (1992) [4] 1279–1283

[7] Mouradoff, L.; et al.: Study of the interaction between liquid aluminum and silicon nitride. J. Europ. Ceram. Soc. **13** (1994) [4] 323–328

[8] Nandy, R.N.; Jogai, R.K.: Selection of proper refractory materials for energy saving in aluminium melting and holding furnaces, Int. J. of Metallurgical Engin. **1** (2012) [6] 117–121

[9] Winston Revie, R.: Uhlig's corrosion handbook. 3rd Ed., Hoboken, NJ, 2011

[10] Routschka, G.; Wuthnow, H.: Praxishandbuch Feuerfeste Werkstoffe, 5th Ed., Essen 2011

[11] Rudolph, S.; Klein, F.: Einsatz von Bornitrid-Schlichten im praktischen Betrieb der Druck- und Kokillengießereien. Gießerei **80** (1993) [8] 256–259

[12] Sarina, B.; Kai, T.; Kvithyld, A.: Wetting of pure aluminium on graphite, SiC and Al_2O_3 in aluminium filtration. Trans. Nonferrous Met. Soc. China **22** (2012) 1930–1938

[13] Schwabe, U.; et al: Corrosion of technical ceramics by molten aluminium. J. Europ. Ceram. Soc. **9** (1992) 407–415

[14] Siljan, O.-J.; et al.: Refractories for molten aluminium contact, Part I: Thermodynamics and kinetics Refractories Applications and News **7** (2002) [6] 17–25

[15] Zhang, Q.; et al.: Adhesion and non-wetting/wetting transition in the Al/Al_2O_3. Interface Phys. Rev. **69** (2004) 045423: 1-11